



HAL
open science

Stress-induced intestinal barrier dysfunction is exacerbated during diet-induced obesity

Wafa Bahlouli, Jonathan Breton, Mauranne Lelouard, Clément L'Huillier, Pauline Tirelle, Emmeline Salameh, Asma Amamou, Karim Atmani, Alexis Goichon, Christine Bole-Feysot, et al.

► To cite this version:

Wafa Bahlouli, Jonathan Breton, Mauranne Lelouard, Clément L'Huillier, Pauline Tirelle, et al.. Stress-induced intestinal barrier dysfunction is exacerbated during diet-induced obesity. *Journal of Nutritional Biochemistry*, 2020, pp.108382. 10.1016/j.jnutbio.2020.108382 . hal-02547813

HAL Id: hal-02547813

<https://normandie-univ.hal.science/hal-02547813v1>

Submitted on 22 Aug 2022

HAL is a multi-disciplinary open access archive for the deposit and dissemination of scientific research documents, whether they are published or not. The documents may come from teaching and research institutions in France or abroad, or from public or private research centers.

L'archive ouverte pluridisciplinaire **HAL**, est destinée au dépôt et à la diffusion de documents scientifiques de niveau recherche, publiés ou non, émanant des établissements d'enseignement et de recherche français ou étrangers, des laboratoires publics ou privés.



Distributed under a Creative Commons Attribution - NonCommercial 4.0 International License

Stress-induced intestinal barrier dysfunction is exacerbated during diet-induced obesity.

Wafa Bahlouli^{1,2}, Jonathan Breton^{1,2}, Mauranne Lelouard^{1,2}, Clément L’Huillier^{1,2}, Pauline Tirelle^{1,2}, Emmeline Salameh^{1,2}, Asma Amamou^{1,2}, Karim Atmani^{1,2}, Alexis Goichon^{1,2}, Christine Bôle-Feysot^{1,2}, Philippe Ducrotté^{1,2,3†}, David Ribet^{1,2}, Pierre Déchelotte^{1,2,4}, Moïse Coëffier^{1,2,4*}.

¹ Normandie University, UNIROUEN, INSERM UMR 1073 “Nutrition, inflammation and gut-brain axis”, 76183 Rouen, France.

² Institute of Research and Innovation in Biomedicine (IRIB), UNIROUEN, 76183 Rouen, France.

³ Department of Gastroenterology, Rouen University Hospital, 76183 Rouen, France

⁴ Department of Nutrition, Rouen University Hospital, 76183 Rouen, France

* Correspondence: moise.coeffier@univ-rouen.fr; Tel.: +33235148240;

Abstract

Obesity and irritable bowel syndrome (IBS) are two major public health issues. Interestingly previous data report a marked increase of IBS prevalence in morbid obese subjects compared with non-obese subjects but underlying mechanisms remain unknown. Obesity and IBS share common intestinal pathophysiological mechanisms such as gut dysbiosis, intestinal hyperpermeability and low-grade inflammatory response. We thus aimed to evaluate the link between obesity and IBS using different animal models. Male C57Bl/6 mice received high fat diet (HFD) for **twenty** weeks and were then submitted to water avoidance stress (WAS). In response to WAS, HFD mice exhibited higher intestinal permeability and plasma corticosterone concentration than non-obese mice. We were not able to reproduce a similar response both in ob/ob mice and in leptin-treated non-obese mice. In addition, metformin, a hypoglycemic agent, limited fasting glycaemia both in unstressed and WAS diet-induced obese mice but only partially restored colonic permeability in unstressed HFD mice. Metformin failed to improve intestinal permeability in WAS HFD mice. Finally, cecal microbiota transplantation from HFD mice in antibiotics-treated recipient mice did not reproduce the effects observed in stressed HFD mice. In conclusion, stress induced a more marked intestinal barrier dysfunction in diet-induced obese mice compared with non-obese mice that seems to be independent of leptin, glycaemia and gut microbiota. These data should be further confirmed and the role of the dietary composition should be studied.

Keywords: morbid obesity, irritable bowel syndrome, gut barrier, leptin, metformin, gut microbiota

Introduction

Obesity, defined by abnormal accumulation of fat and a **body mass index (BMI)** ≥ 30 kg/m², is a significant public health problem in both industrialized and emerging countries. The associated complications, particularly diabetes and cardiovascular diseases, result in the death of at least 2.8 million people each year. In Europe, the prevalence of overweight is estimated approximately at 50% [1] and the prevalence of obesity to be around 16% of the population [2].

Obesity is a multifactorial pathology, linked to genetic, metabolic and environmental factors. Disturbances in the microbiota-gut-brain axis during obesity, in particular intestinal dysbiosis [3, 4] and hyperpermeability [5] have been reported leading to modifications in the regulation of food intake, inflammation and metabolic homeostasis.

Similar mechanisms are also involved in the pathophysiology of irritable bowel syndrome (IBS), a functional gastrointestinal disorder (FGD) defined according to the Rome IV diagnostic criteria by chronic abdominal pain, associated with diarrhea and/or constipation and bloating. The prevalence of IBS is about 5-20% in industrialized countries [6, 7]. IBS is a major public health issue because of a negative impact on the quality of life, the consumption of care and the stops working. The pathophysiology of IBS is multifactorial and includes visceral hypersensitivity, mucosal immune alterations [8], gut dysbiosis [9], enhanced intestinal permeability [10, 11] and psychosocial factors [7].

Some recent studies have suggested a link between obesity and FGDs [12]. A French study showed that the prevalence of IBS was significantly increased (30%) in patients with grade III obesity (BMI>40) [13]. Conversely, in another retrospective study, grade I and II obesity appeared to be associated with reduced risk of IBS [14]. In rodents intestinal occludin expression, a tight junction protein between intestinal epithelial cells, is altered both in diet-induced obese mice [15] and in mice submitted to IBS-like models [16]. Interestingly, in IBS

patients, the expression of occludin, was more severely reduced in patients with BMI > 30 [17]. All these studies highlight a relationship between obesity and IBS, which share pathophysiological factors such as gut dysbiosis, alteration of gut barrier function, low-grade inflammatory response, altered **Toll-like receptors (TLR)** expression but the involved mechanisms remain misunderstood. In addition, stress plays a key role in the pathophysiology of both diseases as recently reviewed [18]. Finally, leptin and plasma glucose may also be involved since both leptin [19] and hyperglycaemia [20] have been shown to regulate gut barrier function.

Taking into account all these data, we thus aimed to better understand the intestinal mechanisms leading to the increased prevalence of IBS in obese subjects. For this purpose, we compared the intestinal response to stress between non-obese, diet-induced and genetically obese mice.

Material and Methods

Animal experimentation

Animal care and experimentation complied with both French and European Community regulations, followed ARRIVE guidelines [21] and the experiment was approved by the Regional Ethical Committee (#6686-2016071512471751 v8). All mice were purchased from Janvier Labs (Genest-St.-Isle, France) and acclimated to the animal facility (controlled temperature ($20 \pm 2^\circ\text{C}$) and with 12 h light–dark cycle) for one week before experimentation. Food and drinking water were free of access.

Water avoidance stress

The water avoidance stress (WAS) model, commonly used to mimic IBS [22], was performed as previously described [16]. Briefly, mice were placed on a small platform in a tank of water (25°C) during **one** hour per day during **ten** consecutive days. Fecal pellet output was monitored during each session. Control mice (C) were kept in standard cages.

Diet-induced and genetic obesity

Six week-old C57Bl/6 male mice were randomized into two groups receiving for **twelve** weeks either standard diet (RM1, SDS France, SD group) or high fat diet (HFD) supplying 60% of calories as fat mainly by lard, 20% as carbohydrates and 20% as protein (#D12492, Research Diets, New Brunswick, NJ). Body weight was measured every two weeks. Two month-old C57Bl/6 male obese *ob/ob* and littermate *ob/-* controls (lean) received standard diet (RM1). Body composition was measured by EchoMRI (EchoMRI, Houston, TX). The first experiment combined diet-induced obesity and WAS leading to four groups (n=10 per group): Standard diet without stress called SD-C; Standard diet and WAS called SD-WAS; High fat diet without stress called HFD-C; High fat diet and WAS called HFD-WAS. The second

experiment combined genetic obesity and WAS leading to **three** groups (n=8 per group): Lean without stress (Lean-C); ob/ob mice without stress (ob/ob – C); ob/ob mice with WAS (ob/ob – WAS)

Leptin experiment:

Seventeen weeks old C57Bl/6 mice were randomized into two groups; treated mice received an i.p. injection of leptin at 10 µg/day (Bachem), as previously described [23], for twenty days (ten days before exposure to WAS and ten days during WAS). The control group received saline. Finally, we obtained three groups (n=8 per group): (1) CT-C; (2) Lept-C; (3) Lept-WAS. All mice had free access to a standard chow and water.

Metformin experiment:

Eight weeks old C57Bl/6 male mice were randomized into two groups receiving for **twelve** weeks either SD or HFD as described above. After **ten** weeks, HFD mice received metformin hydrochloride (500mg, Sigma Aldrich) dissolved in drinking water (wt) at 100 mg/kg/day, as previously described [24], for **twenty** days (**ten** days before the end of the diet and **ten** days during the WAS exposure). The control group received only drinking water. Finally, we obtained six groups (n=8 per group): (1) SD-wt-C; (2) SD-wt-WAS; (3) HFD-wt-C; (4) HFD-wt-WAS; (5) HFD-Met-C; (6) HFD-Met-WAS.

Microbiota experiment:

Donor mice: After **twelve** weeks of SD or HFD (n=10 per group), **eight** weeks old C57Bl/6 mice were euthanized and cecal contents were collected. Cecal contents were then weighed, diluted in sterile phosphate-buffered saline (PBS; 4.75 weight/vol fold dilution) and then centrifuged for 20 sec at 500 rpm. Supernatants were collected and pooled depending on the

respective groups (HFD, SD) and immediately transferred to recipient mice. Remaining aliquots of each cecal content were stored at (-80 ° C) for further bacterial investigations.

Recipient mice: Conventional **eight** weeks old C57Bl/6 mice received by oral gavage (10 µL/g of body weight) a broad spectrum antibiotic cocktail [consisting of ampicillin (10 g/L; Sigma Aldrich), metronidazole (10 g/L; Sigma Aldrich), neomycin trisulfate salt hydrate (10 g/L; Sigma Aldrich), vancomycin hydrochloride hydrate (5 g/L; Sigma Aldrich) and amphotericin B (0.1 g/L; Sigma Aldrich)], twice a day and during **seven** days. To limit the development of fungal species, antifungal solution of amphotericin B (0.1 g/L; Sigma) was administered twice a day over **three** days prior the antibiotic intervention. Twenty-four hours after the last antibiotic cocktail administration, fasted mice received a filtered solution of NaHCO₃ (0.1 g/mL; Sigma Aldrich) 30 min before the cecal microbiota transplant (MT) to counteract the gastric acidity. Then, recipient mice received 200 µl of the respective pools (HFD, SD) of fresh cecal content (240 mg of content/ml) by oral gavage.

Five days after cecal transplantation, recipient mice were exposed or not to WAS. We obtained four groups (n=7-8 per group): (1) SD^{MT}-C; (2) SD^{MT}-WAS; (3) HFD^{MT}-C; (4) HFD^{MT}-WAS.

Glucose tolerance test:

After an overnight fasting with free access to water, mice were i.p. injected with glucose at 1 g/kg of body weight. Blood plasma glucose concentrations were measured from tail vein blood sampling at various times using a FreeStyle Papillon Vision glucometer (Abbott France, Rungis, France). The glucose tolerance test was performed two days before either the beginning of WAS procedure or the beginning of metformin treatment or the cecal content sampling.

Tissue sampling:

Mice were anesthetized with an intraperitoneal injection of ketamine / Largactil (40 and 1 mg. kg⁻¹, respectively). Blood samples were collected, centrifuged (4°C, 3000 rpm, 15 minutes) and plasma was frozen at -80°C. Colonic samples were collected, washed with ice-cold PBS, immediately frozen in liquid nitrogen and stored at -80°C for further analysis. Samples of cecal content and fresh colon were also collected to evaluate microbiota and paracellular permeability, respectively.

Whole intestinal and colonic permeability assessment

At the day 10 of WAS, after a 6-hour fasting period, FITC-dextran (4 kDa, 40 mg/mL) was administered by oral gavage at 10 µL/g of body weight to evaluate the whole intestinal permeability. Three hours later, the last WAS procedure was performed and mice were then immediately euthanized for blood collection. To evaluate colonic paracellular permeability, we used the reference method of Ussing chambers [25] and measured FITC-dextran (4 kDa) fluxes across colonic mucosa as previously described [16]. The fluorescence level of FITC-dextran was then measured either in plasma or in serosal medium with spectrometer Chameleon V (excitation at 485 nm, emission at 535 nm; Hidex, Turku, Finland).

RT-qPCR

Mucosal total RNA was extracted from samples as previously described [26]. After reverse transcription of 1.5 µg total RNA into cDNA by using 200 units of SuperScript™ II Reverse Transcriptase (LifeTechnologies, Cergy-Pontoise, France), qPCR for quantification of pro-inflammatory cytokine (IL-1β, TNF-α) was performed by SYBR™ Green technology on BioRad CFX96 real time PCR system (BioRad Laboratories, Marnes la Coquette, France) in

duplicate for each sample. GAPDH was used as the endogenous reference gene and primers have been previously detailed [16].

Quantitative analysis of bacterial communities in cecal content

Total genomic DNA from each cecal samples was extracted using Qiagen QIAamp DNA stool kit, following a protocol including a bead-beating step [27]. DNA was eluted in 200 μ l of Tris-EDTA buffer (10 mM Tris HC, pH 8, 0.5 mM EDTA) and quantified with a Nanodrop® 2000 / 2000c spectrophotometer (NanoDrop Technologies, Wilmington, DE, US). Quantitative real-time polymerase chain reaction (qPCR) was then performed on these DNA samples using Itaq Universal SYBR Green Supermix (BioRad) for detection and primers amplifying the 16S rRNA genes [28, 29] from Eubacteria (Eub-338F: ACTCCTACGGGAGGCAGCAG, Eub-518R: ATTACCGCGGCTGCTGG), Firmicutes (Firm-F: ATGTGGTTTAATTCGAAGCA, Firm-R: AGCTGACGACAACCATGCAC) and Bacteroidetes (Bact-F: CATGTGGTTTAATTCGATGAT, Bact-R: AGCTGACGACAACCATGCAG). All samples were run in duplicate in 96-well reaction plates. Final concentrations were as follow: DNA (0.1 ng/ μ L, expect for *A. muciniphila* 1 ng/ μ L), primers 0.5 μ M, and SYBR Green Supermix 1X. Serial dilution of DNA from cecal content was included on each plate to generate a relative curve and to integrate primer efficiency in the calculations.

Western blot analysis

Colonic mucosa was homogenized in ice-cold lysis buffer containing 0.1% protease inhibitor cocktail (Sigma Aldrich) and western blot was performed as previously described [30]. Briefly, proteins (25 μ g) were separated on 4-20% glycine resolving gels (Biorad Laboratories) and transferred to a nitrocellulose membrane (GE Healthcare, Orsay, France), which was

blocked for 1 hour at room temperature with 5% (w/v) non-fat dry milk in Tris Buffered Saline (TBS) (10 mmol/L Tris, pH 8; 150 mmol/L NaCl), plus 0.05% (w/v) Tween 20. Then, an overnight incubation at 4°C was performed with anti-occludin or anti-claudin 1 (1:1000, LifeTechnologies) or with mouse anti- β -actin (1:1000, Sigma Aldrich) antibodies. After three washes in a blocking solution of 5% (w/v) non-fat dry milk in TBS/0.05% and Tween 20, a 1 hour incubation with peroxidase-conjugated goat anti-rabbit or anti-mouse IgG (1:5000; Dako) was performed. After three additional washes, immuno-complexes were revealed using the Enhanced ChemiLuminescence (ECL) detection system (GE Healthcare). Protein bands were quantified by densitometry using ImageScanner III and ImageQuant TL software (GE Healthcare).

Corticosterone assay

Corticosterone was measured using a commercial serum corticosterone enzyme immunoassay kit according to the manufacturer's instructions (Abnova, Ann Arbor, MI).

Statistical analysis

Statistical analysis was performed using GraphPad Prism 5.0 (GraphPad software Inc, San Diego, CA, USA). To compare two groups, t-test or Mann-Whitney test was used, as appropriate. If variances significantly differed between groups (Bartlett's test) or if normality test was not passed (Kolmogorov-Smirnov test), Mann-Whitney test was performed. To compare three groups or conditions, statistical analysis consisted in two-way ANOVA (WAS x Treatment (TT)) followed by Bonferroni post-tests. For all tests, $p < 0.05$ was considered significant.

Results

After **twelve** weeks, HFD induced a gain of 17.8 g in body weight compared to 7.5 g for the SD. This increase was only related to an increase of fat mass. Lean mass remained unchanged between HFD and SD groups (Figure 1A). Ob/ob mice showed higher body weight than HFD mice, as well as higher percentage of fat mass (Figure 1B, C). HFD mice had higher fasting glycaemia compared with SD and ob/ob mice (Figure 1D) even if both HFD and ob/ob mice showed glucose intolerance (Figure 1E, F). Indeed, plasma glucose was increased at 15, 30, 60 and 90 min in HFD mice and at 15, 60 and 90 min in ob/ob mice compared with SD.

We have then submitted HFD mice to WAS. To evaluate colonic motility, we monitored the number of output feces during WAS procedure. As expected for this model of stress, HFD and SD mice showed an increase of output feces number in response to WAS compared to HFD-C and SD-C, respectively (Figure 2A). However, the number of output feces was lower in HFD-WAS than in SD-WAS. Ob/ob mice showed a similar response with an increase of colonic motility in response to WAS (Figure 3A). Serum corticosterone was unchanged in SD-WAS compared to SD-C that is in accordance with previous data [16] and in HFD mice (Figure 2B). By contrast, HFD-WAS mice exhibited a marked increase of serum corticosterone compared with other groups. Both ob/ob-C and ob/ob-WAS mice had an increase of corticosterone compared with lean mice (Figure 3B). To evaluate whole intestinal permeability, mice were administered by oral gavage with FITC-dextran 4kDa that was then measured in plasma. Plasma FITC-D concentration was increased in HFD-C mice (+37%) but more markedly in HFD-WAS mice (+152%) compared with SD (Figure 2C). Indeed, HFD-WAS exhibited a significant increase of plasma FITC-D compared to other 3 groups suggesting that combination of both obesity and stress have a stronger effect on intestinal permeability than obesity alone. However, In ob/ob mice, we did not observe a similar pattern, since plasma FITC-D concentration remained unaffected both in ob/ob-C and ob/ob-

WAS groups (Figure 3C). We then focused on colon to evaluate paracellular permeability by Ussing chambers. We observe a trend for an increase in colonic permeability in SD-WAS compared to SD, but difference did reach significance ($p=0.085$). HFD mice exhibited a similar increase in colonic permeability whatever the presence of WAS or not (Figure 2D). Again, ob/ob mice showed different response compared to HFD. A trend for a decrease of colonic permeability was observed in ob/ob-C mice ($p=0.095$) whereas ob/ob-WAS exhibited higher colonic permeability than in ob/ob-C (+84%, $p<0.05$) but similar to lean-C group (Figure 3D). These discrepancies may be explained by different alterations of tight junction protein expression. Occludin expression was reduced in SD-WAS, HFD-C and HFD-WAS groups compared with SD-C (Figure 2E) while both occludin and claudin-1 expression remained unchanged in ob/ob mice (Figure 3E, F). IL-1 β mRNA level, used as a marker of inflammatory response, was increased in HFD-C and HFD-WAS mice compared with SD-C (Figure 2F). We did not observe difference between HFD-C and HFD-WAS groups. Ob/ob mice did not show any significant difference for IL-1 β (Figure 3G).

As HFD and ob/ob mice showed different pattern of response to WAS and exhibited different fasting glycaemia (Figure 1D), we choose to focus on the role of leptin and glycaemia.

To evaluate the role of leptin, we injected wild type C57Bl/6 mice with leptin to reproduce increased plasma level of leptin in diet-induced obese mice. Leptin treatment did not affect body weight (data not shown). During WAS, leptin-treated mice exhibited increased number of output feces (Figure 4A), but no modification of plasma corticosterone concentration (data not shown), of whole intestinal permeability evaluated by plasma FITC-D (Figure 4B) and colonic permeability (Figure 4C). In accordance, tight junction protein expression (occludin and claudin-1) remained unaffected (data not shown). Leptin-treated mice only showed increased colonic IL-1 β mRNA in response to WAS (Figure 4D). All these data suggest that observed effects in diet-induced obese mice were independent of leptin pathway.

To evaluate the putative role of glycaemia in the regulation of intestinal permeability in HFD mice during WAS, we performed an additional experiment in HFD mice treated or not with Metformin for **twenty** days. Similarly to the previous experiment, HFD induced body weight gain (Figure 5A) related to fat mass gain (Figure 5B). HFD mice exhibited higher fasting glycaemia and glucose intolerance compared with SD mice (Figure 5 C, D). After **twenty** days of metformin treatment, HFD mice showed a partial restoration of fasting glycaemia in both mice submitted to WAS (HFD-met-WAS) or not (HFD-Met-C). In mice submitted to WAS, fasting glycaemia was significantly reduced after metformin treatment compared to HFD-wt-WAS (Figure 6B). Interestingly, WAS induced a weight loss in both SD and HFD mice but metformin blunted body weight loss (Figure 6A). The number of output feces increased in SD-wt-WAS and HFD-wt-WAS mice compared with SD-wt-C and HFD-wt-C, respectively, as observed in the first experiment (Figure 6C). In metformin-treated mice, we observed an increase of output feces in both mice submitted to WAS or not (Figure 6C), suggesting an enhanced colonic motility in metformin-treated mice. Plasma corticosterone concentration was affected by WAS procedure ($p(\text{WAS}) = 0.006$, two-way ANOVA) but metformin had no effect (Figure 6D). Similarly, whole intestinal permeability was affected by WAS ($p(\text{WAS}) = 0.046$, two-way ANOVA) without effect of metformin treatment (Figure 6E). Both WAS and HFD induced an increase of colonic paracellular permeability (Figure **7A**). Interestingly, metformin partially restored colonic permeability only in HFD-Met-C mice but not in HFD-Met-WAS mice. However, metformin was not able to restore tight junction protein expression, occludin and claudin-1, in the colon of mice submitted or not to WAS (Figure **7B, C**). Concerning colonic inflammatory response, metformin only restored IL-1 β mRNA level in HFD mice submitted to WAS (Figure **7D**).

Thus, our data showed that leptin injections were not able to mimic HFD mice response to WAS and that metformin treatment did not reduce intestinal permeability, suggesting that

other mechanisms or pathways should be involved. We then evaluated the putative effects of gut microbiota. For this purpose, we performed microbiota transplantation (MT) experiment.

A third experiment was done with HFD that reproduced previous data with higher body weight gain (Figure 8A) and glucose intolerance (Figure 8B and C) in HFD mice than in SD mice. In addition, HFD mice also exhibited increased colonic permeability compared with SD (Figure 8D). Cecal contents of SD and HFD mice were then taken and transferred to antibiotic-treated recipient mice. After five days, recipient mice were then submitted or not to WAS.

Mice receiving microbiota from SD (SD^{MT}) tended to lose body weight in response to WAS whereas mice receiving microbiota from HFD (HFD^{MT}) showed a trend for an increase. Consequently, body weight change was significantly different between SD^{MT} -WAS and HFD^{MT} -WAS groups (Figure 9A). In response to WAS, both SD^{MT} and HFD^{MT} exhibited an increase of the number of output feces (Figure 9B), while plasma corticosterone concentration remained unaffected (Figure 9C). Surprisingly, in response to WAS, we observed that whole intestinal permeability (Figure 9D) and colonic permeability (Figure 9E) decreased in both SD^{MT} and HFD^{MT} groups ($p(WAS) < 0.05$, two-way ANOVA). Colonic occludin expression was only reduced in HFD^{MT} -WAS mice compared to other groups (Figure 9F). Colonic claudin-1 expression (Figure 9G) and IL-1 β mRNA (Figure 9H) were increased in SD^{MT} -WAS and HFD^{MT} -C compared with SD^{MT} -C but not in HFD^{MT} -WAS. Mice receiving microbiota from HFD donor mice did not reproduce the phenotype of HFD mice in response to WAS while MT seemed to be effective. Indeed, eubacteria were reduced both in HFD donor mice and in mice receiving microbiota from HFD (Figure 10 A-B). In addition, the *Firmicutes* / *Bacteroidetes* ratio, which was increased in HFD donor mice, remained higher in recipient mice ($p(HFD) = 0.041$, two-way ANOVA, Figure 10 C,D)

Discussion

In the present study, we report that diet-induced obesity exacerbates intestinal hyperpermeability in response to stress that may partially explain the increased prevalence of IBS previously reported in severe obese patients [13]. In addition, our data also suggest that neither leptin nor glycaemia contribute to this response, as well as gut microbiota.

Recently, Schneck et al reported that the prevalence of IBS increased to 30% in severe obese patients [13] compared to 4.7% in general population in France [6]. Even if obesity and IBS share pathophysiological mechanisms at the intestinal level, this increased prevalence remains unexplained. In the present study, we showed that HFD mice submitted to WAS model exhibited both increased intestinal permeability, compared to obese mice and to non-obese WAS mice, and increased plasma corticosterone levels. Previous data showed that both HFD-induced obesity [15] and WAS [16, 22] are associated with increased intestinal permeability. In IBS patients, increased intestinal permeability has been described in many studies [11, 31-33] with alterations both in the small intestine [34, 35] and in the colon [10, 17, 36]. In obese patients, increased intestinal permeability has also been reported in some studies [5, 37]. Interestingly, we previously showed that colonic occludin expression was more markedly decreased in obese IBS patients compared with non-obese IBS patients [17]. However, in the present study, colonic permeability was mainly affected by obesity and colonic occludin expression was similarly reduced in WAS, obese and WAS-obese mice. Interestingly, ob/ob mice did not reproduce the results observed in HFD mice. Intestinal permeability was not increased in ob/ob mice compared with littermate controls. Those data are in accordance with previous paper showing no difference of intestinal permeability between ob/ob mice and wild type mice of the same strain [38] while enhanced permeability has been reported in other papers [39, 40]. However, leptin injections were not able to reproduced HFD-induced intestinal hyperpermeability. Again, published data are controversial since leptin has been

shown to increase paracellular permeability *in vitro* [41, 42] but leptin alleviated gut barrier function *in vivo* [43]. Le Dréan et al speculate that leptin may have different effects on intestinal permeability whether leptin binds its receptor on apical or basal epithelial side [19]. These data suggest that leptin pathway are not involved in the specific HFD mice response to stress.

Then, we focused on the role of glycaemia since HFD mice exhibited glucose intolerance but also high fasting glycaemia. In addition, Thaïss et al recently reported that hyperglycaemia drives intestinal barrier dysfunction [20]. Metformin is a widely-used drug that results in clear benefits in relation to glucose metabolism and diabetes-related complications [44]. In our study, metformin partially restored fasting glycaemia and colonic permeability in unstressed HFD mice. Recent data underlined that metformin reduced epithelial paracellular permeability in Caco-2 cells [45], or *in vivo* during inflammatory [46, 47] and stress models [48, 49]. Nevertheless, in our study, metformin failed to improve intestinal permeability in stressed HFD mice that was not yet described to our knowledge.

Finally, we choose to focus on gut microbiota since gut dysbiosis has been reported both in IBS [9] and obese patients [50]. Cecal microbiota transplantation from HFD mice in antibiotics-treated recipient mice did not reproduce the effects observed in stressed HFD mice suggesting that the gut microbiota did not trigger the exacerbation of intestinal permeability in stressed HFD mice. Interestingly, the prevalence rates of dysbiosis has been evaluated in IBS patients with and without morbid obesity [51]. In this latter study, the authors reported higher rates of dysbiosis in groups with morbid obesity whatever the presence or not of IBS.

Our study has some limitations. First, we used a diet with 60% of kcal from fat that is commonly used in rodents [52, 53] but that is higher than western diet. The influence of different amounts of fat should be further investigated. **Second, we only used the water-avoidance stress model because of previously paper from our lab [16]. However, other stress**

models have been previously used to mimic IBS-like symptoms by others such as the forced swim test [54], restraint stress [55], maternal separation model [56] or chronic acute combined stress [57]. These data should be further reproduced in these models. Third, we were not able to determine the exact mechanisms involved in the exacerbation of intestinal permeability occurring in stressed HFD mice. Leptin pathway and glycaemia seem to be not involved. However, dose-dependent effects and the route of leptin and metformin administrations may explain the absence of specific effects on intestinal permeability, even if both leptin and metformin treatments have been effectively confirmed by colonic IL-1 β and glycaemia changes, respectively. In addition, our data should be confirmed by using other approaches like germ-free mice for instance. Finally, in the present study, due to the high fat diet, WAS procedure was performed in five months old mice. We cannot exclude that the response to WAS could be different compared to younger mice [16, 22].

Conclusion

In conclusion, stress induces a more marked intestinal barrier dysfunction in diet-induced obese mice compared with non-obese mice that seems to be independent of leptin, glycaemia and gut microbiota. The exacerbated intestinal barrier dysfunction may contribute to the increase of IBS prevalence in morbid obese patients. These data should be further confirmed and the role of diet composition should be investigated.

Acknowledgements

This work was co-supported by the Microbiome foundation, the Roquette foundation for health and by European Union and Normandie Regional Council (to W.B. and for equipment). Europe gets involved in Normandie with European Regional Development Fund

(ERDF). These funders did not participate in the design, implementation, analysis, and interpretation of the data.

Author contributions

WB, JB, ML, CL, PT, ES, AA, KA, AG, CBF and DR performed experiments and analyses.

WB, PDU and MC designed experiments. WB, DR, PDe and MC interpreted the data. WB and MC wrote the main manuscript text and prepared figures. All authors reviewed the manuscript.

References

1. Gallus, S., et al., *Overweight and obesity in 16 European countries*. Eur J Nutr, 2015. **54**(5): p. 679-89.
2. Marques, A., et al., *Prevalence of adult overweight and obesity in 20 European countries, 2014*. Eur J Public Health, 2018. **28**(2): p. 295-300.
3. Turnbaugh, P.J., et al., *Diet-induced obesity is linked to marked but reversible alterations in the mouse distal gut microbiome*. Cell Host Microbe, 2008. **3**(4): p. 213-23.
4. Cani, P.D., et al., *Changes in gut microbiota control metabolic endotoxemia-induced inflammation in high-fat diet-induced obesity and diabetes in mice*. Diabetes, 2008. **57**(6): p. 1470-81.
5. Teixeira, T.F., et al., *Intestinal permeability parameters in obese patients are correlated with metabolic syndrome risk factors*. Clin Nutr, 2012. **31**(5): p. 735-40.
6. Le Pluart, D., et al., *Functional gastrointestinal disorders in 35,447 adults and their association with body mass index*. Aliment Pharmacol Ther, 2015. **41**(8): p. 758-67.
7. Ford, A.C., B.E. Lacy, and N.J. Talley, *Irritable Bowel Syndrome*. N Engl J Med, 2017. **376**(26): p. 2566-2578.
8. Bashashati, M., et al., *Colonic immune cells in irritable bowel syndrome: A systematic review and meta-analysis*. Neurogastroenterol Motil, 2018. **30**.
9. Menees, S. and W. Chey, *The gut microbiome and irritable bowel syndrome*. F1000Res, 2018. **7**.
10. Piche, T., et al., *Impaired intestinal barrier integrity in the colon of patients with irritable bowel syndrome: involvement of soluble mediators*. Gut, 2009. **58**(2): p. 196-201.
11. Dunlop, S.P., et al., *Abnormal intestinal permeability in subgroups of diarrhea-predominant irritable bowel syndromes*. Am J Gastroenterol, 2006. **101**(6): p. 1288-94.
12. Pickett-Blakely, O., *Obesity and irritable bowel syndrome: a comprehensive review*. Gastroenterol Hepatol (N Y), 2014. **10**(7): p. 411-6.
13. Schneck, A.S., et al., *Increased Prevalence of Irritable Bowel Syndrome in a Cohort of French Morbidly Obese Patients Candidate for Bariatric Surgery*. Obes Surg, 2016. **26**(7): p. 1525-30.
14. Carter, D., et al., *Predictive factors for the diagnosis of irritable bowel syndrome in a large cohort of 440,822 young adults*. J Clin Gastroenterol, 2015. **49**(4): p. 300-5.

15. de La Serre, C.B., et al., *Propensity to high-fat diet-induced obesity in rats is associated with changes in the gut microbiota and gut inflammation*. *Am J Physiol Gastrointest Liver Physiol*, 2010. **299**(2): p. G440-8.
16. Ghouzali, I., et al., *Targeting immunoproteasome and glutamine supplementation prevent intestinal hyperpermeability*. *Biochim Biophys Acta*, 2017. **1861**(1 Pt A): p. 3278-3288.
17. Bertiaux-Vandaële, N., et al., *The expression and the cellular distribution of the tight junction proteins are altered in irritable bowel syndrome patients with differences according to the disease subtype*. *Am J Gastroenterol*, 2011. **106**: p. 2165-73.
18. Pugliese, G., et al., *Irritable bowel syndrome: a new therapeutic target when treating obesity?* *Hormones (Athens)*, 2019.
19. Le Drean, G. and J.P. Segain, *Connecting metabolism to intestinal barrier function: The role of leptin*. *Tissue Barriers*, 2014. **2**(4): p. e970940.
20. Thaiss, C.A., et al., *Hyperglycemia drives intestinal barrier dysfunction and risk for enteric infection*. *Science*, 2018. **359**(6382): p. 1376-1383.
21. Kilkenney, C., et al., *Survey of the quality of experimental design, statistical analysis and reporting of research using animals*. *PLoS One*, 2009. **4**(11): p. e7824.
22. Goichon, A., et al., *Colonic Proteome Signature in Immunoproteasome-Deficient Stressed Mice and Its Relevance for Irritable Bowel Syndrome*. *J Proteome Res*, 2019. **18**(1): p. 478-492.
23. Maurya, R., et al., *Differential Role of Leptin as an Immunomodulator in Controlling Visceral Leishmaniasis in Normal and Leptin-Deficient Mice*. *Am J Trop Med Hyg*, 2016. **95**(1): p. 109-119.
24. Zhou, Z.Y., et al., *Metformin exerts glucose-lowering action in high-fat fed mice via attenuating endotoxemia and enhancing insulin signaling*. *Acta Pharmacol Sin*, 2016. **37**(8): p. 1063-75.
25. Herrmann, J.R. and J.R. Turner, *Beyond Ussing's chambers: contemporary thoughts on integration of transepithelial transport*. *Am J Physiol Cell Physiol*, 2016. **310**(6): p. C423-31.
26. Coeffier, M., et al., *Increased Proteasome-Mediated Degradation of Occludin in Irritable Bowel Syndrome*. *Am J Gastroenterol*, 2010. **105**(5): p. 1181-1188.
27. Costea, P.I., et al., *Towards standards for human fecal sample processing in metagenomic studies*. *Nat Biotechnol*, 2017. **35**(11): p. 1069-1076.
28. Queipo-Ortuno, M.I., et al., *Gut microbiota composition in male rat models under different nutritional status and physical activity and its association with serum leptin and ghrelin levels*. *PLoS One*, 2013. **8**(5): p. e65465.
29. Fierer, N., et al., *Assessment of soil microbial community structure by use of taxon-specific quantitative PCR assays*. *Appl Environ Microbiol*, 2005. **71**(7): p. 4117-20.
30. Jesus, P., et al., *Alteration of intestinal barrier function during activity-based anorexia in mice*. *Clin Nutr*, 2014. **33**: p. 1046-53.
31. Zhou, Q., B. Zhang, and G.N. Verne, *Intestinal membrane permeability and hypersensitivity in the irritable bowel syndrome*. *Pain*, 2009. **146**(1-2): p. 41-6.
32. Zhou, Q., et al., *Randomised placebo-controlled trial of dietary glutamine supplements for postinfectious irritable bowel syndrome*. *Gut*, 2018.
33. Spiller, R.C., et al., *Increased rectal mucosal enteroendocrine cells, T lymphocytes, and increased gut permeability following acute Campylobacter enteritis and in post-dysenteric irritable bowel syndrome*. *Gut*, 2000. **47**(6): p. 804-11.
34. Martinez, C., et al., *The jejunum of diarrhea-predominant irritable bowel syndrome shows molecular alterations in the tight junction signaling pathway that are associated with mucosal pathobiology and clinical manifestations*. *Am J Gastroenterol*, 2012. **107**(5): p. 736-46.
35. Martinez, C., et al., *Diarrhoea-predominant irritable bowel syndrome: an organic disorder with structural abnormalities in the jejunal epithelial barrier*. *Gut*, 2013. **62**(8): p. 1160-8.

36. Annahazi, A., et al., *Luminal Cysteine-Proteases Degrade Colonic Tight Junction Structure and Are Responsible for Abdominal Pain in Constipation-Predominant IBS*. *Am J Gastroenterol*, 2013. **108**(8): p. 1322-31.
37. Damms-Machado, A., et al., *Gut permeability is related to body weight, fatty liver disease, and insulin resistance in obese individuals undergoing weight reduction*. *Am J Clin Nutr*, 2017. **105**(1): p. 127-135.
38. Stenman, L.K., et al., *Genetically obese mice do not show increased gut permeability or faecal bile acid hydrophobicity*. *Br J Nutr*, 2013. **110**(6): p. 1157-64.
39. Nagpal, R., et al., *Obesity-Linked Gut Microbiome Dysbiosis Associated with Derangements in Gut Permeability and Intestinal Cellular Homeostasis Independent of Diet*. *J Diabetes Res*, 2018. **2018**: p. 3462092.
40. Johnson, A.M., et al., *High fat diet causes depletion of intestinal eosinophils associated with intestinal permeability*. *PLoS One*, 2015. **10**(4): p. e0122195.
41. Kim, C.Y. and K.H. Kim, *Curcumin prevents leptin-induced tight junction dysfunction in intestinal Caco-2 BBe cells*. *J Nutr Biochem*, 2014. **25**(1): p. 26-35.
42. Le Drean, G., et al., *Visceral adipose tissue and leptin increase colonic epithelial tight junction permeability via a RhoA-ROCK-dependent pathway*. *FASEB J*, 2014. **28**(3): p. 1059-70.
43. Ye, C., et al., *Leptin alleviates intestinal mucosal barrier injury and inflammation in obese mice with acute pancreatitis*. *Int J Obes (Lond)*, 2018. **42**(8): p. 1471-1479.
44. Rena, G., D.G. Hardie, and E.R. Pearson, *The mechanisms of action of metformin*. *Diabetologia*, 2017. **60**(9): p. 1577-1585.
45. Zhou, H.Y., et al., *Metformin regulates tight junction of intestinal epithelial cells via MLCK-MLC signaling pathway*. *Eur Rev Med Pharmacol Sci*, 2017. **21**(22): p. 5239-5246.
46. Chen, L., et al., *Activating AMPK to Restore Tight Junction Assembly in Intestinal Epithelium and to Attenuate Experimental Colitis by Metformin*. *Front Pharmacol*, 2018. **9**: p. 761.
47. Deng, J., et al., *Metformin protects against intestinal barrier dysfunction via AMPKalpha1-dependent inhibition of JNK signalling activation*. *J Cell Mol Med*, 2018. **22**(1): p. 546-557.
48. Nozu, T., et al., *Metformin inhibits visceral allodynia and increased gut permeability induced by stress in rats*. *J Gastroenterol Hepatol*, 2019. **34**(1): p. 186-193.
49. Li, Y., et al., *Metformin prevents colonic barrier dysfunction by inhibiting mast cell activation in maternal separation-induced IBS-like rats*. *Neurogastroenterol Motil*, 2019. **31**(5): p. e13556.
50. Cotillard, A., et al., *Dietary intervention impact on gut microbial gene richness*. *Nature*, 2013. **500**(7464): p. 585-8.
51. Aasbrenn, M., J. Valeur, and P.G. Farup, *Evaluation of a faecal dysbiosis test for irritable bowel syndrome in subjects with and without obesity*. *Scand J Clin Lab Invest*, 2018. **78**(1-2): p. 109-113.
52. François, M., et al., *High-fat diet increases ghrelin-expressing cells in stomach, contributing to obesity*. *Nutrition*, 2016. **32**: p. 709-15.
53. Gomez-Zorita, S., et al., *Relationship between Changes in Microbiota and Liver Steatosis Induced by High-Fat Feeding-A Review of Rodent Models*. *Nutrients*, 2019. **11**(9).
54. Zhao, Y.J., et al., *Extracellular signal-regulated kinase activation in the spinal cord contributes to visceral hypersensitivity induced by craniofacial injury followed by stress*. *Neurogastroenterol Motil*, 2018. **30**(2).
55. Agostini, S., et al., *A marketed fermented dairy product containing Bifidobacterium lactis CNCM I-2494 suppresses gut hypersensitivity and colonic barrier disruption induced by acute stress in rats*. *Neurogastroenterol Motil*, 2012. **24**(4): p. 376-e172.
56. Miquel, S., et al., *Anti-nociceptive effect of Faecalibacterium prausnitzii in non-inflammatory IBS-like models*. *Sci Rep*, 2016. **6**: p. 19399.
57. Yu, Y., et al., *The effect of curcumin on the brain-gut axis in rat model of irritable bowel syndrome: involvement of 5-HT-dependent signaling*. *Metab Brain Dis*, 2015. **30**(1): p. 47-55.

Figure legends

Figure 1: Body weight, body composition and glycaemia in mice with diet-induced or genetic obesity. Changes in body weight, fat mass and lean mass in mice receiving standard diet (SD, open bars) or high fat diet (HFD, blue bars) during **twelve** weeks (A). Body weight (B.), body composition (C.) and fasting glycaemia (D.) in mice receiving SD (n=20), HFD (n=20) or in ob/ob mice (n=16). Glycaemia (E.) and area under the curve of glycaemia (F.) in response to i.p. glucose tolerance test in mice receiving SD, HFD or in ob/ob mice. *, p<0.05; **, p<0.01; ***, p<0.001. (E.) values without a common letter significantly differ, p<0.05.

Figure 2: Response to water avoidance stress in mice with diet-induced obesity. Output feces number (A.), plasma corticosterone (B.) and plasma FITC-dextran 4kDa (C.) measured in mice (n=10 per group) receiving during **twelve** weeks standard diet (SD) or high fat diet (HFD) and submitted to water avoidance stress (WAS) or not (c). Colonic samples were obtained and placed in Ussing chambers or immediately frozen. Serosal side concentrations of FITC-dextran 4kDa of colonic samples placed in Ussing chambers (D.), colonic occludin expression (E.) and IL-1 β mRNA level (F.) in mice receiving during **twelve** weeks SD or HFD and submitted to WAS or not. Values without a common letter significantly differ, p<0.05.

Figure 3: Response to water avoidance stress in mice with genetic obesity. Output feces number (A.), plasma corticosterone (B.) and plasma FITC-dextran 4kDa (C.) measured in lean and ob/ob mice (n=8 per group) submitted to water avoidance stress (WAS) or not (c). Colonic samples were obtained and placed in Ussing chambers or immediately frozen. Serosal side concentrations of FITC-dextran 4kDa of colonic samples placed in Ussing chambers (D.), colonic occludin (E.) and claudin-1 expression (F.) and IL-1 β mRNA level (G.) in lean and ob/ob mice submitted to WAS or not. Values without a common letter significantly differ, p<0.05.

Figure 4: Response to water avoidance stress in mice receiving leptin injections. Output feces number (A.) and plasma FITC-dextran 4kDa (B.) measured in mice (n=8 per group) receiving during **twenty** days i.p. injections of vehicle (CT) or leptin (Lept) and submitted to water avoidance stress (WAS) or not (c). Colonic samples were obtained and placed in Ussing chambers or immediately frozen. Serosal side concentrations of FITC-dextran 4kDa of colonic samples placed in Ussing chambers (C.) and colonic IL-1 β mRNA level (D.) in vehicle or leptin treated mice submitted to WAS or not. Values without a common letter significantly differ, p<0.05.

Figure 5: Body weight, body composition and glucose tolerance in diet-induced obese mice. Body weight (A.) and body composition (B.) in mice receiving standard diet (SD, n=16) or high fat diet (HFD, n=32) during **ten** weeks. Glycaemia (C.) and area under the curve of glycaemia (D.) in response to i.p. glucose tolerance test in mice receiving SD or HFD. ***, p<0.001 vs SD

Figure 6: Systemic response to water avoidance stress in diet-induced obese mice receiving metformin injections. Body weight changes (A.), fasting glycaemia (B.), output feces number (C.), plasma corticosterone (D.) and plasma FITC-dextran 4kDa (E.) measured in mice (n=8 per group) receiving standard diet (SD) or high fat diet (HFD) during **twelve** weeks, receiving drinking water alone (wt) or with metformin (Met) and submitted to water

avoidance stress (WAS) or not (c). Values without a common letter significantly differ, $p < 0.05$.

Figure 7: Colonic response to water avoidance stress in diet-induced obese mice receiving metformin injections. Colonic samples were obtained from mice ($n=8$ per group) receiving standard diet (SD) or high fat diet (HFD) during twelve weeks, receiving drinking water alone (wt) or with metformin (Met) and submitted to water avoidance stress (WAS) or not (c). Colonic samples placed in Ussing chambers or immediately frozen. Serosal side concentrations of FITC-dextran 4kDa of colonic samples placed in Ussing chambers (A.), colonic occludin (B.) and claudin-1 expression (C.) and IL-1 β mRNA level (D.) in mice receiving SD or HFD during twelve weeks, receiving or not Met and submitted or not to WAS. Values without a common letter significantly differ, $p < 0.05$.

Figure 8: Body weight, body composition, glucose tolerance and colonic paracellular permeability in diet-induced obese mice used as microbiota donors. Body weight (A.), glucose tolerance test (B., C.) and plasma FITC-dextran 4 kDa in mice receiving standard diet (SD) or high fat diet (HFD) during twelve weeks ($n=10$ per group). (A-D) **, $p < 0.01$; ***, $p < 0.001$ vs SD.

Figure 9: Response to water avoidance stress in mice receiving cecal microbiota from diet-induced obese mice. Body weight changes (A.), output feces number (B.), plasma corticosterone (C.), and plasma FITC-dextran 4kDa (D.) measured in mice receiving cecal microbiota from SD (SD^{MT}) or HFD (HFD^{MT}) mice and then submitted to water avoidance stress (WAS) or not (c) ($n=7-8$ per group). Colonic samples were obtained and placed in Ussing chambers or immediately frozen. Serosal side concentrations of FITC-dextran 4kDa of colonic samples placed in Ussing chambers (E.), colonic occludin (F.) and claudin-1 expression (G.) and IL-1 β mRNA level (H.) in SD^{MT} and HFD^{MT} mice submitted or not to WAS. Values without a common letter significantly differ, $p < 0.05$.

Figure 10: Eubacteria and Firmicutes/Bacteroidetes ratio in mice receiving cecal microbiota from diet-induced obese mice. Donor mice received either standard diet (SD) or high fat diet (HFD) during twelve weeks. Recipient mice (SD^{MT} and HFD^{MT}) were gavaged with cecal microbiota from SD or HFD donor mice and were then submitted to water avoidance stress (WAS) or not (c). Eubacteria (A. and B.) and Firmicutes/Bacteroidetes (C. and D.) ratio measured by qPCR in cecal content from donor ($n=10$ per group) and recipient ($n=7-8$ per group) mice, respectively. (A, C) *, $p < 0.05$ vs SD. (B, D) values without a common letter significantly differ, $p < 0.05$.

Figure 1

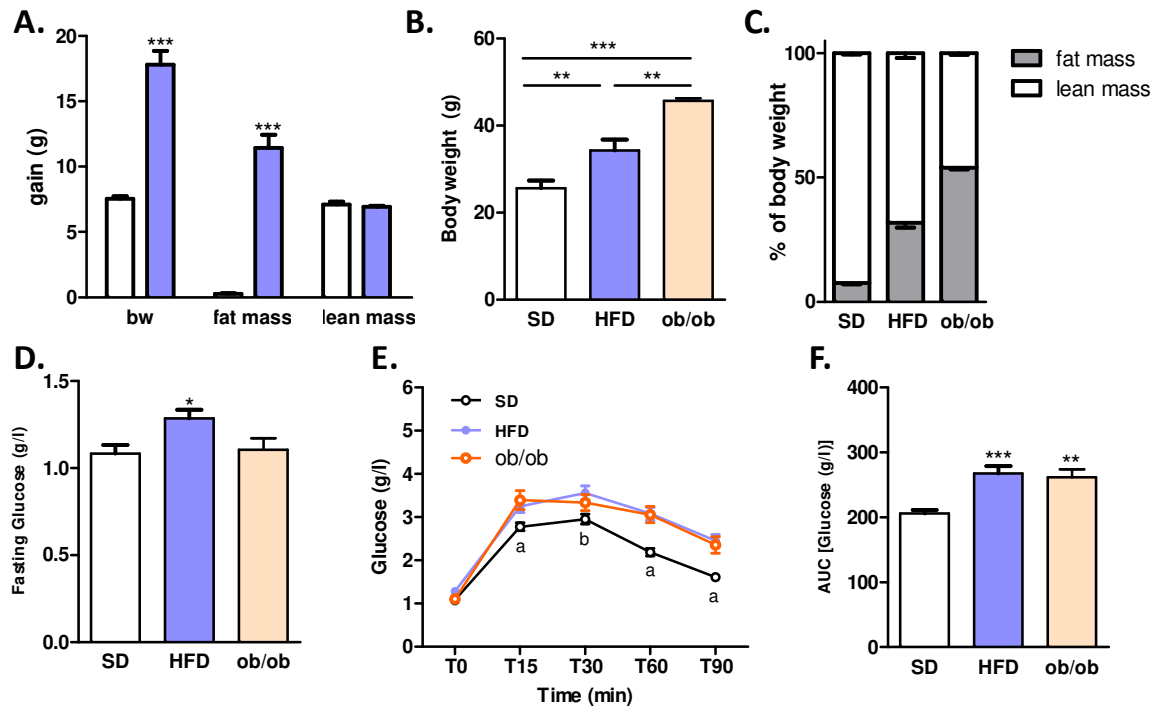


Figure 2

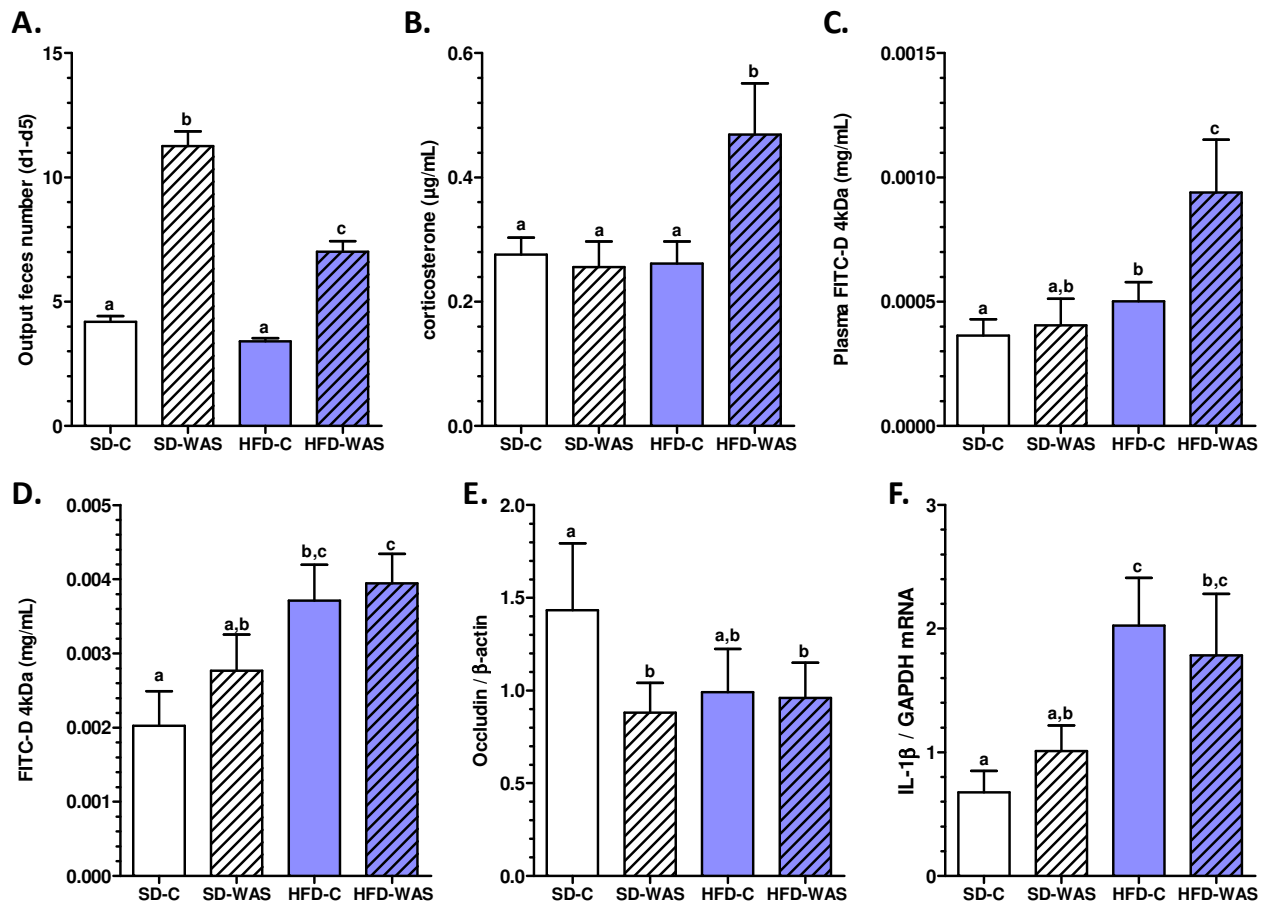


Figure 3

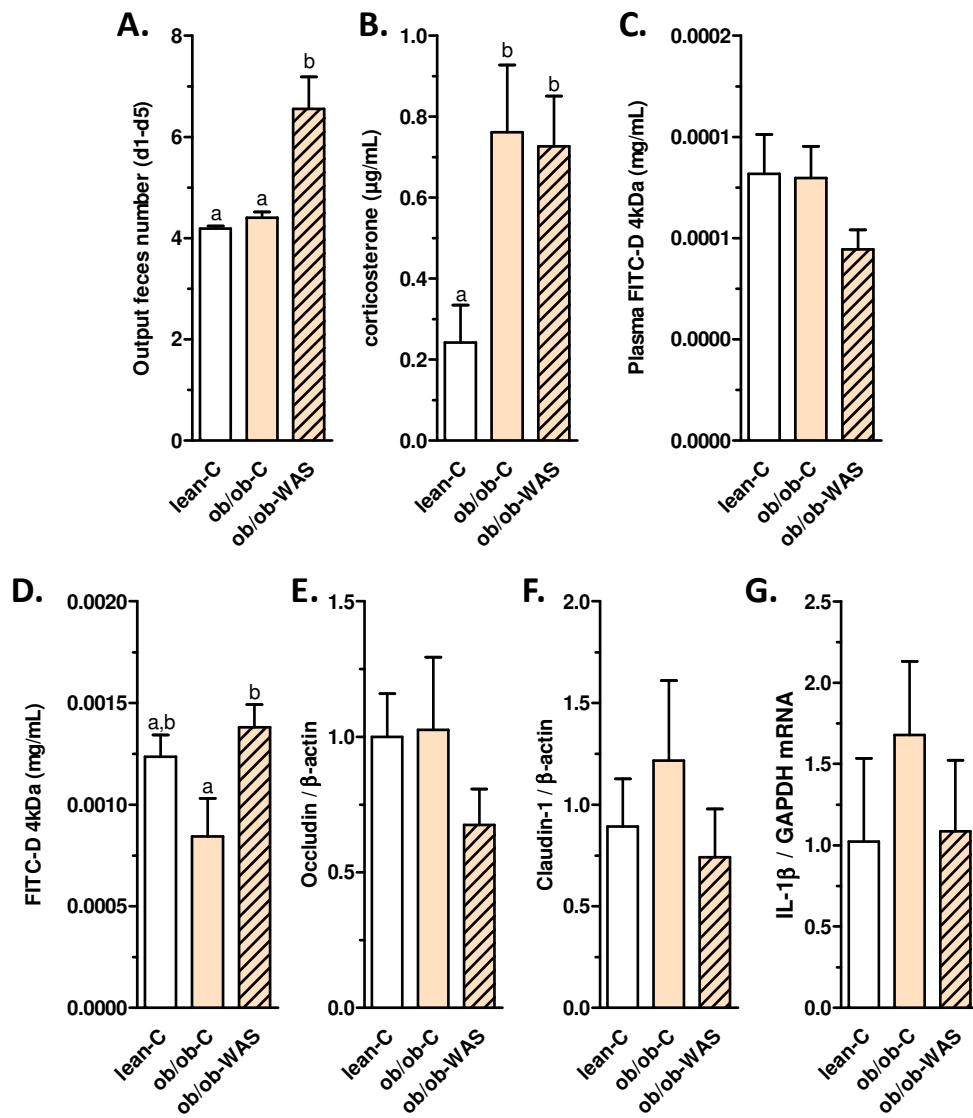


Figure 4

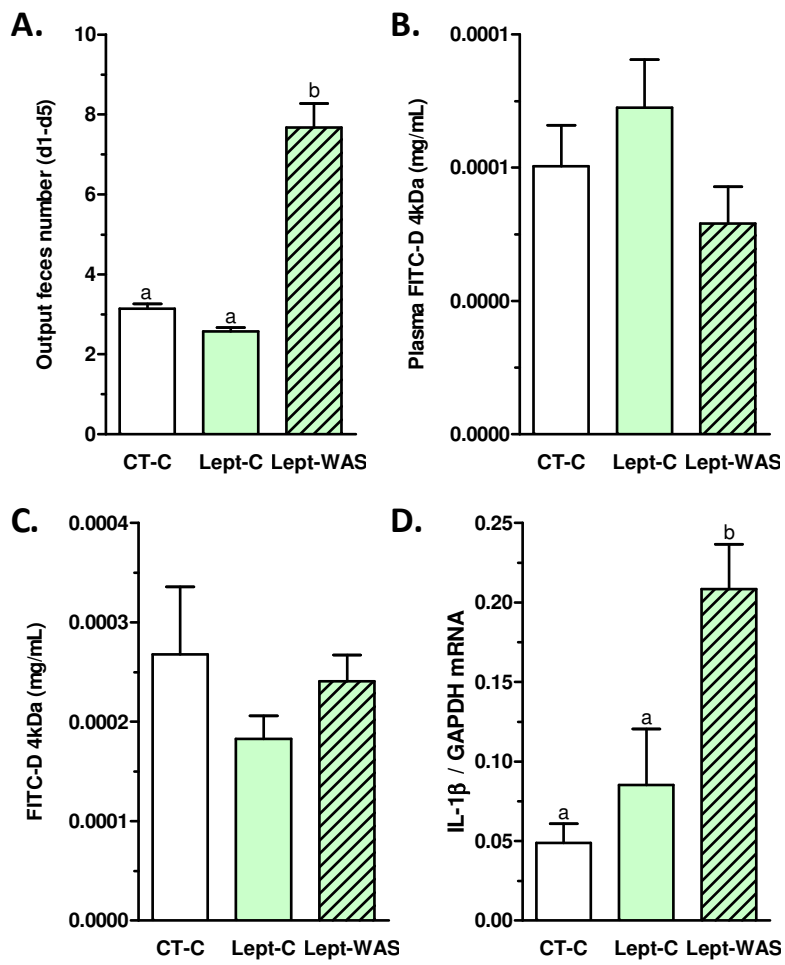


Figure 5

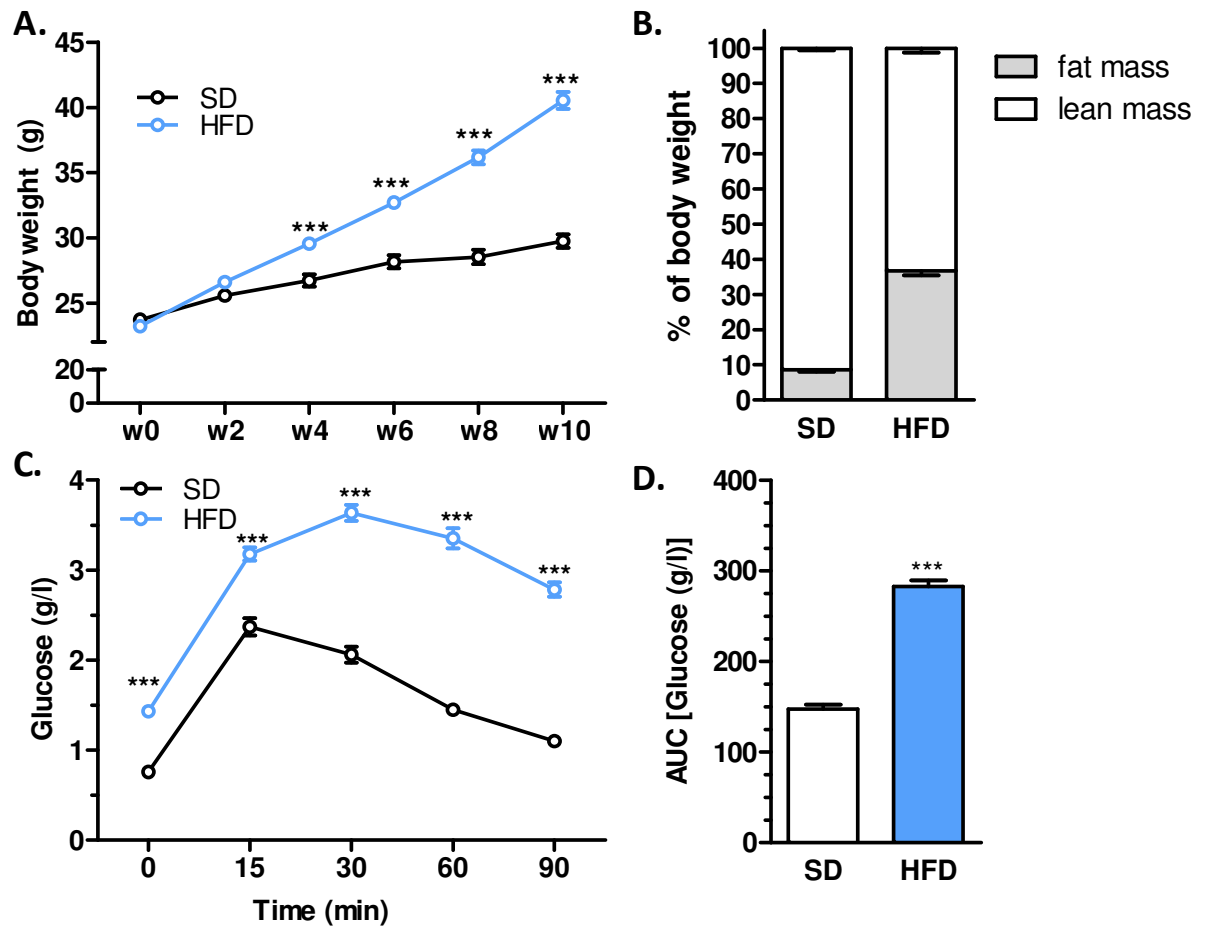


Figure 6

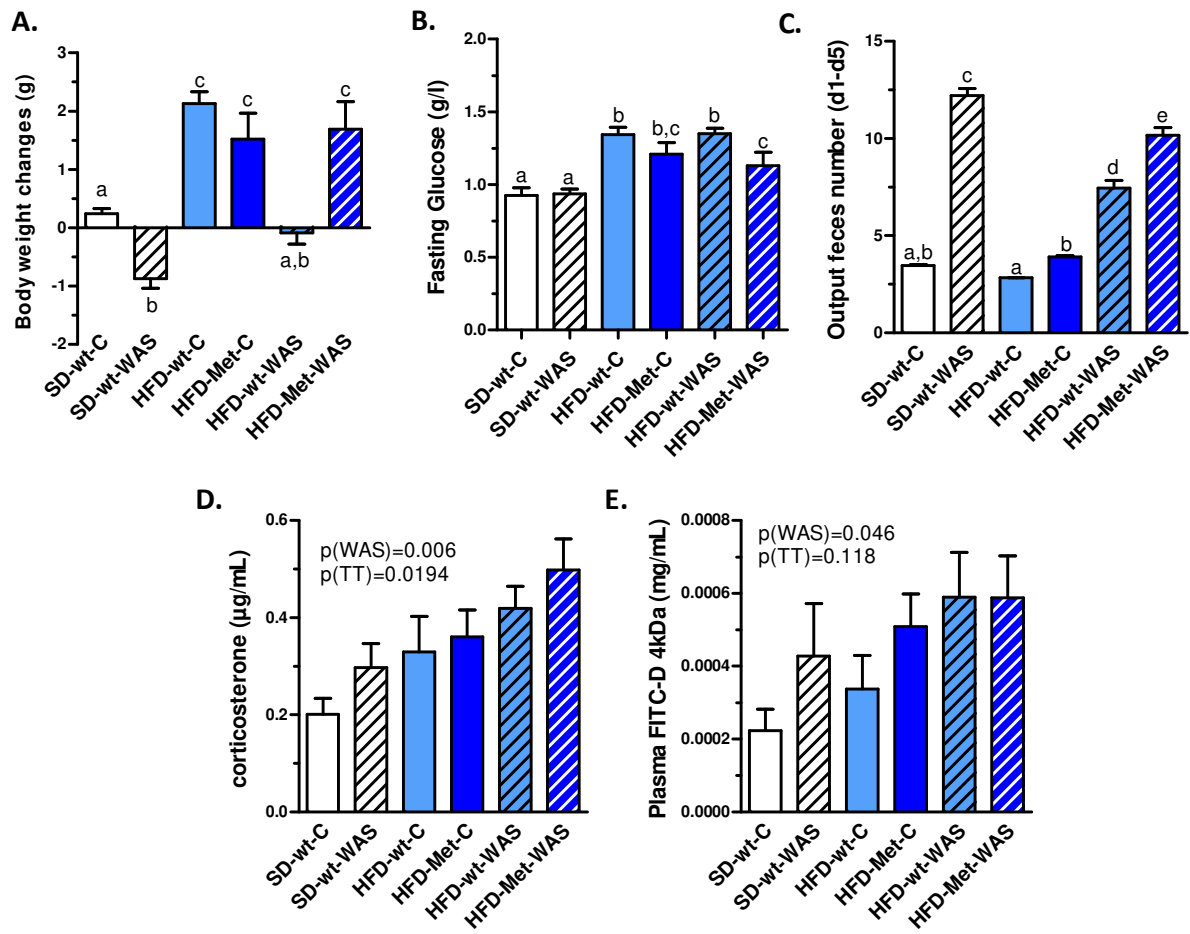


Figure 7

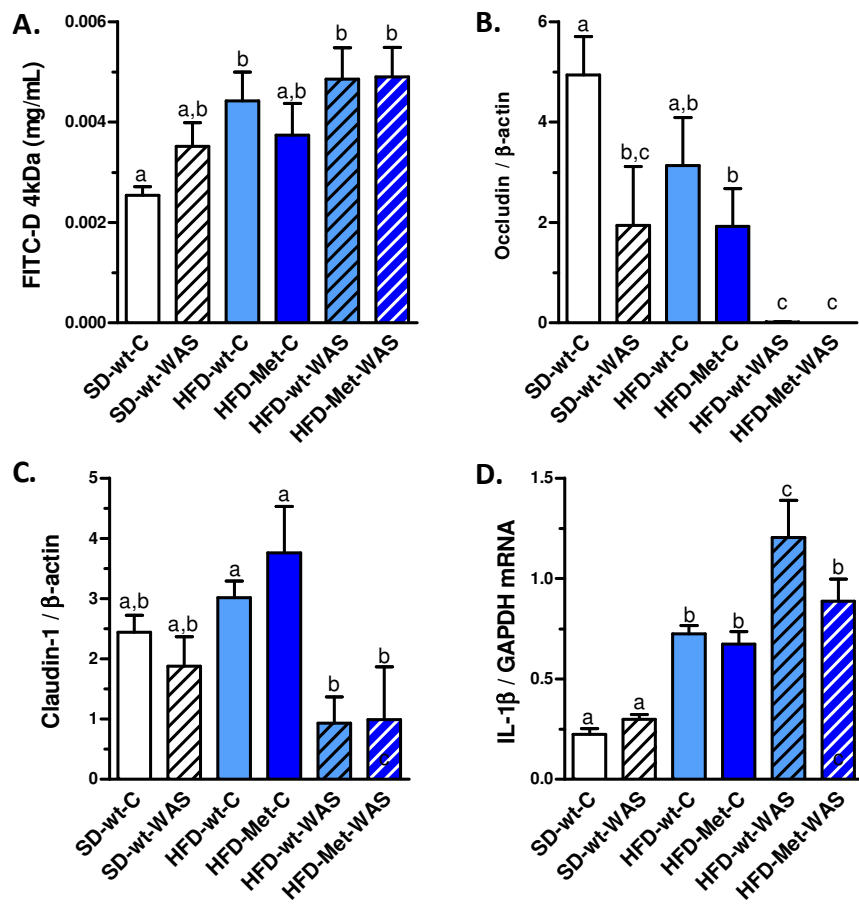


Figure 8

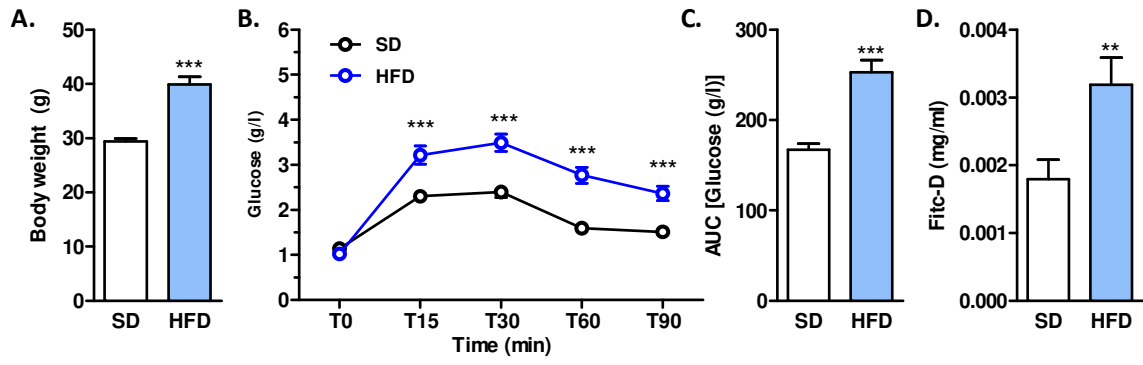


Figure 9

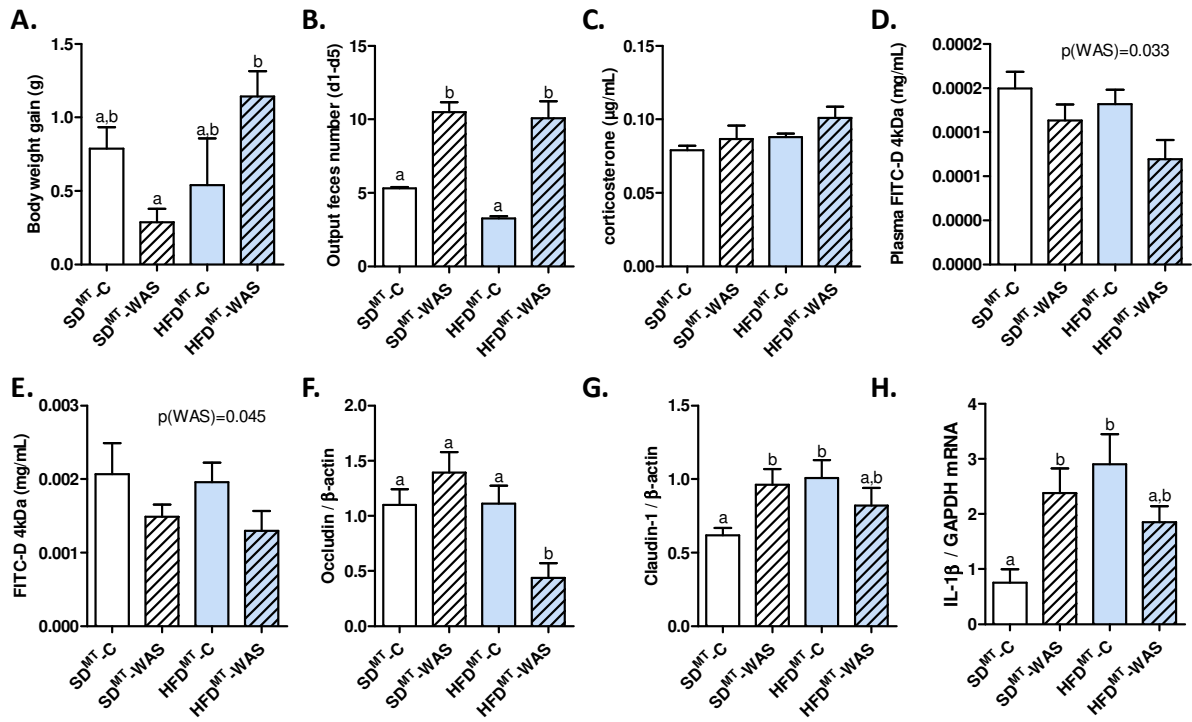


Figure 10

